Department for Biomedical Sciences

University of Veterinary Medicine Vienna

Institute of Laboratory Animal Science

(Head: Univ.-Prof. Dr. Thomas Rülicke)

Recombination efficiency of the Cre-loxP system at the murine *Ing3* locus

Bachelor Thesis

for obtaining the degree

Bachelor of Science (BSc)

University of Veterinary Medicine Vienna

submitted by

Viktor Lang

Vienna, June 2020

Scientific Supervisor:	**Dipl.-Ing. Dr. nat. techn. Dieter Fink**
Reviewer:	**Ao. Univ.-Prof. Dr. rer. nat. Marina Karaghiosoff**

Contents

1 Introduction

1.1 *ING3*: status in health and cancer

The inhibitor of growth 3 (*ING3*) gene belongs to a family of tumour suppressors encompassing five members (*ING1-5*), with the candidate tumour suppressor *ING3* being the most evolutionarily distinctive (He et al. 2005). The founding member, *ING1*, was discovered through differential screening between the transcriptome of normal mammary epithelial cells and breast cancer cells (Garkavtsev et al. 1996). Later, *ING2-5* genes were found by applying bioinformatic approaches based upon sequence homology (Nagashima et al. 2001, 2003, Shiseki et al. 2003).

ING proteins share multiple highly conserved domains, such as a plant homeodomain (PHD) and a nuclear localization signal (He et al. 2005), indicating similar biological functions. The PHD is an epigenetic reader module recognizing methylated lysine 4 residues of histone H3, marking transcriptional start sites (Liang et al. 2004, Shi et al. 2006).

ING3 acts as a stoichiometric component of the nucleosome acetyltransferase of histone H4 (NuA4) complex, an evolutionarily conserved multi-subunit histone acetyltransferase (HAT), capable of adding acetyl groups to histone H4 and H2A N-terminal tails (Doyon et al. 2004). By recruiting the NuA4 complex, ING3 directs HAT activity to the appropriate chromatin substrates. Dynamic chromatin remodelling processes have major implications on gene-specific transcription regulation. Acetylation of chromatin loosens the interaction between histones and DNA, thereby increasing chromatin accessibility and gene expression. Alterations in the maintenance and propagation of epigenetic modifications can give rise to the initiation and progression of various cancers, depending on the genomic context (Berger 2007).

Similarly to ING1, the candidate tumour suppressor ING3 acts as a negative growth regulator and enhances p53-dependent transcription (Nagashima et al. 2003). For instance, ING3 has been shown to enhance activity of the cyclin-dependent kinase inhibitor 1 promoter, ultimately resulting in cell cycle arrest predominantly at the G1/S transition (Kataoka et al. 2003). Differential expression of ING3 at the mRNA level in cell lines facing varying levels of reactive oxygen species may point towards a role in sensing harmful stimuli (Kitahara et al. 2003). ING3 expression is strongly enhanced after UV irradiation in a p53-independent manner, followed by activation of the Fas/caspase-8 pathway, thus linking genotoxic stress to apoptosis (Wang and Li 2006).

Taking all these factors into account, it is reasonable to predict an involvement of ING3 dysregulation in tumourigenesis and neoplastic growth. Downregulation of ING3 expression at the mRNA level has been linked to human head and neck cancers (Gunduz et al. 2002) and hepatocellular carcinoma (Lu et al. 2012), while reduced nuclear ING3 localization was reported to be a key indicator of human cutaneous melanoma progression (Wang et al. 2007).

However, with the rise of more reliable immunological tools, high ING3 expression has been associated with a wide-range of rapidly proliferating human tissues, including small intestine, bone marrow and epidermis (Nabbi et al. 2015). In contrast to its putative tumour suppressor status in the types of cancer mentioned above, recent studies assign *ING3* an oncogenic role in prostate cancer, based on a higher survival rate of human prostate cancer patients with lower ING3 levels (Almami et al. 2016). This notion was supported by experimental data linking ING3 expression to induction of cellular proliferation in *ex vivo* benign prostate hyperplasia tissue (McClurg et al. 2018).

Activation of the androgen receptor (AR) is an important mediator of prostate cancer pathogenesis. Upon binding androgenic hormones, the AR translocates into the nucleus and regulates the transcription of several target genes. The AR is a known substrate of the NuA4 complex. By physically interacting with both the AR and the NuA4 complex in the cytoplasm, ING3 directs HAT activity to the immediate vicinity of the AR, enhancing AR activation and nuclear translocation, resulting in the development and progression of prostate cancer (Nabbi et al. 2017).

1.2 Murine *Ing3* knockout models

Recently, a murine ubiquitous *Ing3* mutant mouse model was characterized. Briefly, a reporter cassette has integrated into the *Ing3* locus and disrupted and inactivated the *Ing3* gene. Homozygous mutants were embryonically lethal, displaying growth retardation and impaired brain development, suggesting an important role in neuroectoderm development (Fink et al. 2020).

Prior to this study, germline-competent C57BL/6N embryonic stem cells (EUCOMM clone EPD0028_2_H09) harbouring the reporter-tagged *Ing3*$^{tm1a(EUCOMM)Wtsi}$ knockout-first allele (*Ing3*-tm1a allele; Mouse Genome Informatics ID: 4432585) were injected into SWISS blastocytes and backcrossed to C57BL/6N (Barones et al., manuscript in preparation).

In brief, the *Ing3*-tm1a allele is comprised of a promoterless beta-galactosidase (*lacZ*)-tagged selection cassette flanked by flippase recognition target (FRT) sites. Flippase (FLP) catalyses recombination events between pairs of FRT signals (Broach et al. 1982). In addition, loxP (locus of crossover in P1) sequences are inserted at either side of a critical exon of the *Ing3* gene. The Cre-loxP system is a well characterized genomic engineering tool with cyclization recombinase (Cre) facilitating site-specific excision of DNA sequences flanked by two loxP recognition sites (floxed) in the same orientation (Sternberg and Hamilton 1981). Successive exposure to FLP and Cre triggers the removal of the reporter cassette (tm1a to tm1c allele) and deletion of the critical exon (tm1c to tm1d allele; SKARNES et al. 2011). Hereafter, *Ing3*^{fl} represents the *Ing3*-tm1c allele, *Ing3*$^{\Delta}$ the *Ing3*-tm1d allele and *Ing3*$^{+}$ the wildtype *Ing3* allele. Figure 1 summarizes mutant allele nomenclature, allele conversion and underlying recombination events.

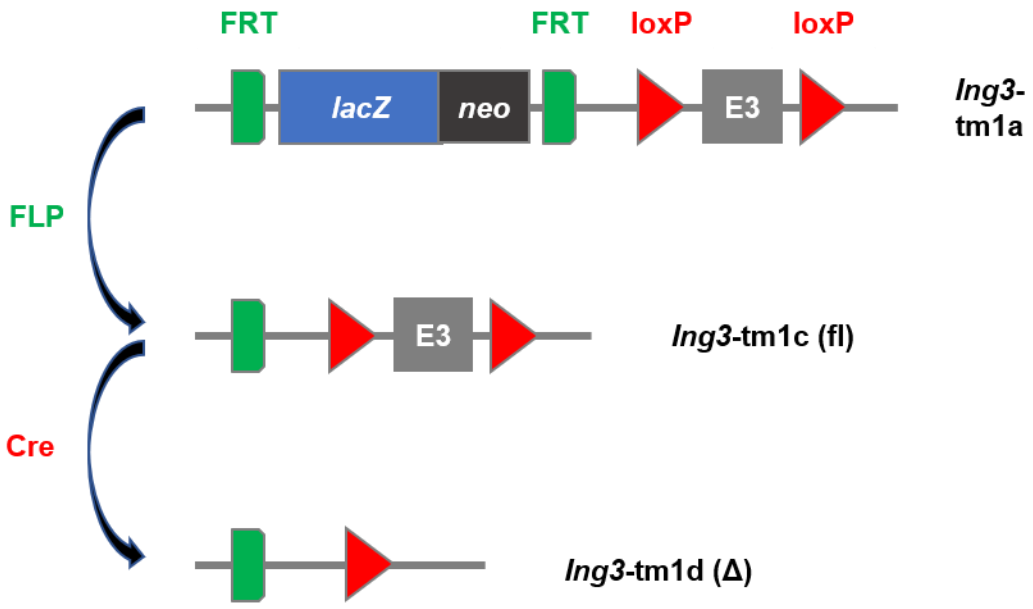

Figure 1. Schematic representation of the European Conditional Mouse Mutagenesis (EUCOMM) program alleles. FLP-mediated recombination deletes the *lacZ*-tagged selection cassette, while Cre recombinase catalyses the excision of a critical exon, thus disrupting *Ing3* function. (FLP: flippase recombinase, Cre: cyclization recombinase, FRT: FLP recognition target, loxP: Cre recognition target, *lacZ*: beta-galactosidase reporter, *neo*: neomycin resistance gene, E3: critical exon 3 of *Ing3*; adapted by permission from Springer Nature: Skarnes et al. 2011. A conditional knockout resource for the genome-wide study of mouse gene function. Nature, 474(7351):337–342, © 2011. License Number: 4807040839989)

1.3 Basic principles of digital PCR and immunohistochemistry

Digital PCR (dPCR) is a powerful and increasingly affordable technique that allows absolute quantification of nucleic acid sequences (Vogelstein and Kinzler 1999). The approach involves partitioning of the sample into a large number of distinct reaction chambers, followed by PCR amplification. An end-point fluorescent signal generated by a hydrolysis probe (or dye) is measured by a reader instrument (Sundberg et al. 2010). Absolute quantification of the target sequence is achieved by applying a Poisson error correction to the ratio of positive partitions to total number of partitions (Vogelstein and Kinzler 1999).

Immunohistochemistry (IHC), a versatile tool utilising the interactions between enzyme-labelled antibodies and specific antigens, has been developed in the early 20th century. After visualizing the immunoreaction, the distribution of an antigen can be assessed in tissue sections (Coons et al. 1941).

1.4 Aim of this thesis

In order to study the effects of *Ing3* inactivation in prostate cancer development in adult mice, a prostate-specific Cre-loxP induced *Ing3* knockout mouse model was established. This was achieved by cross-breeding female carriers of the *Ing3*-tm1c allele to male mice bearing the PB-Cre4 transgene, which directs Cre expression to the epithelial lining of the prostatic glands (Wu et al. 2001). In order to confirm recombination success and assess the recombination efficiency in the prostatic glands, dPCR was performed. For calibration of the dPCR and to confirm the embryonic lethal phenotype of *Ing3* in a full knockout mouse model, yet another ubiquitous *Ing3* knockout line was generated, utilising the female PB-Cre4 mouse as an efficient global deleter (Birbach 2013). Furthermore, I performed immunohistochemistry on mouse prostate glands to assess ING3 depletion.

2 Materials and Methods

2.1 Animal care and husbandry

Mice were housed in a specific pathogen-free environment in compliance with FELASA recommendations (Mahler Convenor et al. 2014). Regular mouse diet (ssniff Spezialdiäten, Soest, Germany) and water was provided *ad libitum*. Surrounding temperature and relative humidity were monitored and regulated (temperature: 22 °C ± 1 °C; relative humidity: 50% ± 10 percentage points). A maximum of five mice depending on age were kept in individually ventilated cages (Eurostandard Type IIL; Tecniplast, Buguggiate, Italy) with adequate enrichment and nesting material.

Animal handling and health monitoring was performed by trained animal caretakers and the scientific investigators. All procedures adhered to all federal, state and local laws on animal experimentation (animal breeding license number: BMWFW-68.205/0049-WF/V/3b/2015) and regulations issued by the Ethics and Animal Welfare Committee of the University of Veterinary Medicine Vienna, Austria (ETK-011/01/2020).

2.2 Animal breeding scheme

Prior to this study, *Ing3*-tm1c mice were obtained by FLP-mediated conversion of the C57BL/6N-Ing3$^{tm1a(EUCOMM)Wtsi}$/Biat strain. In order to obtain prostate-specific *Ing3* knockout mice, the PB-Cre4 transgene (Tg(Pbsn-cre)4Prb, JAX stock number 026662) was inherited by the male (Figure 2A).

For the generation of a ubiquitous *Ing3* knockout model, female PB-Cre4 transgenic mice were utilised as global Cre deleters. To produce viable homozygous *Ing3* knockout offspring, ING3 expression was reconstituted by crossbreeding to an ING3 overexpressing transgenic mouse line, designated as C57BL/6N-TgTn(sb-CAG-Ing3-P2A-eGFP)774.1Biat and hereafter referred to as CAG-Ing3-P2A-eGFP (Fink et al. 2020) (Figure 2B).

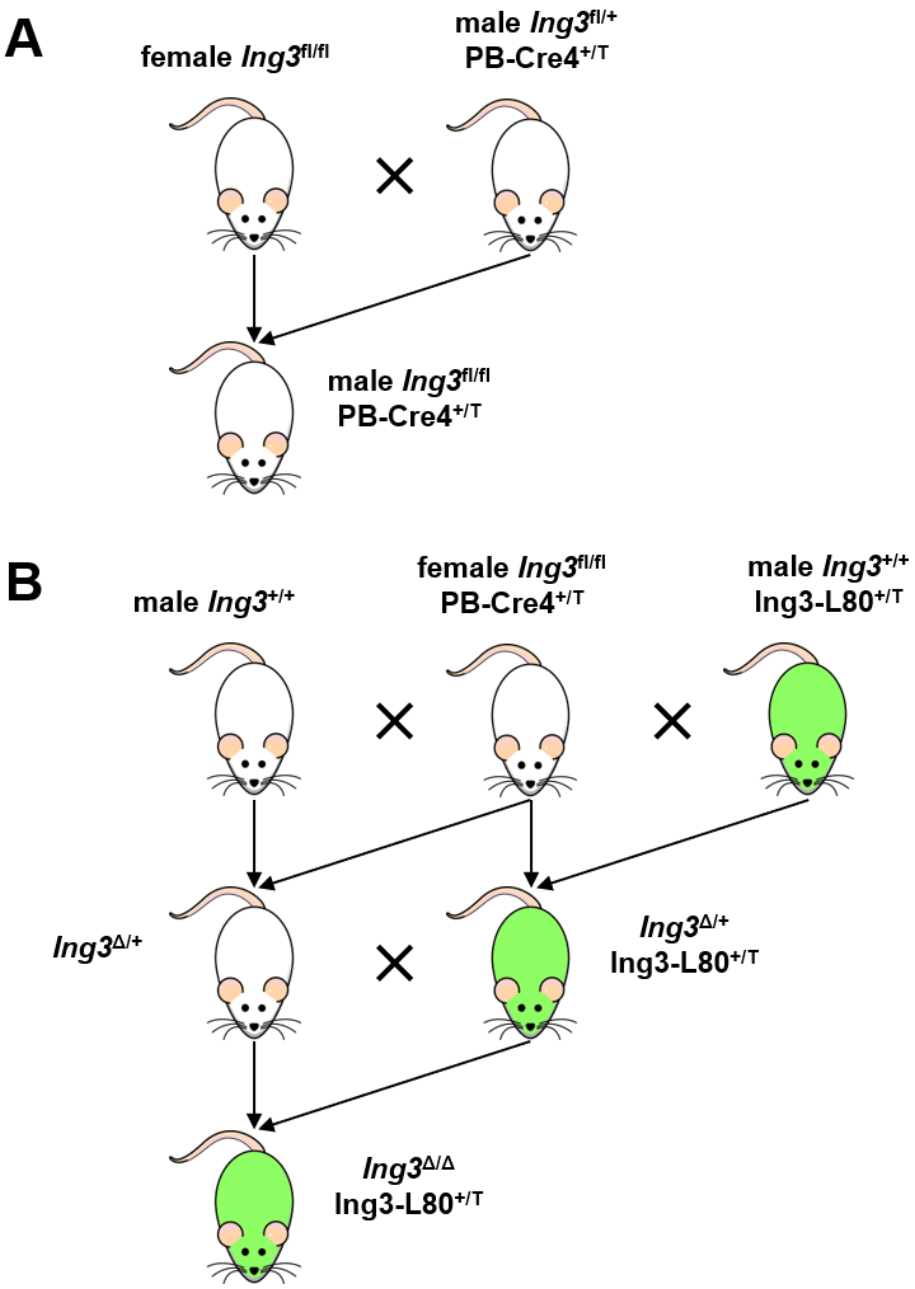

Figure 2. Schematic scheme of mouse breeding. (A) Generation of a prostate-specific conditional *Ing3* knockout mouse. **(B)** Generation of a ubiquitous *Ing3* knockout mouse. Murine *Ing3* is mapped to chromosome 6qA3.1. The *Ing3* expression vector of the CAG-Ing3-P2A-eGFP mouse line (Ing3-L80) integrated into chromosome 12, whereas the PB-Cre4 transgene is located on chromosome 11. (PB-Cre4$^{+/T}$: PB-Cre4 positive mouse)

2.3 Tissue sampling and processing

Upon weaning at approximately 21 days after birth, ear notching was performed for identification of the animal. The ear notch was collected and subjected to DNA extraction and subsequent genotyping by means of conventional PCR. Prostate-specific *Ing3* knockout mice were sacrificed by cervical dislocation, followed by immediate harvest of prostate tissue samples and disposal of animal carcasses.

For dPCR analysis, the anterior, dorsolateral and ventral lobes of the prostate were isolated and subjected to DNA extraction. For IHC, the prostate was removed *en bloc* together with the urethra and immersed in 10% formalin (catalogue number: 9713.1000; VWR International, Radnor, Pennsylvania, USA) overnight and then placed in 70% ethanol. Brain, kidney and liver tissue samples of a male wildtype mouse were included as positive controls for ING3 staining. Paraffin embedding was carried out by the Work Group of Histology and Embryology, Department of Pathobiology (University of Veterinary Medicine, Vienna, Austria). PB-Cre4 negative control groups were implemented in both dPCR and IHC.

2.4 DNA extraction

Tissue samples were immersed in 98 µl TNES buffer (10 mM Tris-HCl, 400 mM NaCl, 100 mM EDTA, 0.6% SDS) and 2 µl Proteinase K (catalogue number: EO0491; Thermo Scientific™, division of Thermo Fisher Scientific, Dreieich, Germany) and digested overnight at 55 °C. Next, 35 µl of 5 M NaCl was added and mixed thoroughly by vortexing. After centrifugation in a benchtop centrifuge at high speed (12,000–14,000 × g) for five minutes at room temperature to pellet cell debris, the supernatant was transferred to a fresh microcentrifuge tube. DNA was precipitated by adding 100 µl of ice-cold 96% ethanol, followed by gently mixing through inverting the tubes and centrifugation at high speed for five minutes. Immediately after centrifugation the supernatant was discarded by decanting. The precipitate was rinsed with 500 µl 70% ethanol and centrifuged at high speed for five minutes. All liquids were removed by gently decanting. The DNA pellet was air-dried until residual ethanol had evaporated and resuspended overnight at room temperature in 100 µl Tris-EDTA buffer (10 mM Tris-HCl, 1 mM EDTA, pH 8). DNA was stored at -4 °C until further processing.

2.5 PCR genotyping

Primers were designed by Dr. Dieter Fink using the free plasmid sequence editor tool ApE (version 2.0.50; https://jorgensen.biology.utah.edu/wayned/ape/) and synthesised as

standard, desalted DNA oligonucleotides (Sigma-Aldrich, Steinheim am Albuch, Germany). Primer designations and sequences are listed in Table 1. The primers Cre-Forward and Cre-Reverse amplify a 434-bp amplicon in mice harbouring the PB-Cre4 transgene (Table 2, PCR program 1). The CAG-Ing3-P2A-eGFP transgenic construct can be detected with primers LSL-CAG-Forward and LSL-Ing3-Reverse, producing a 337-bp fragment (Table 2, PCR program 2). PCR amplification using the primers Ing3-floxed-Forward and Ing3-floxed-Reverse yields a 250-bp band for the wildtype *Ing3* allele and a 413-bp band for the *Ing3*-tm1c allele (Table 2, PCR program 1). Cre-mediated conversion of the *Ing3*-tm1c allele into the *Ing3*-tm1d allele is detected by primers Ing3-floxed-Forward and Ing3-genomic-Reverse, which amplify a 293-bp amplicon for the *Ing3*-tm1d allele, a 1108-bp amplicon for the *Ing3*-tm1c allele and a 929-bp amplicon for the wildtype allele of *Ing3* (Table 2, PCR program 3).

Table 1: Primers for PCR genotyping.

Primer designation	**Primer sequence (5'–3')**
LSL-CAG-Forward	GCCTCTGCTAACCATGTTCATGC
LSL-Ing3-Reverse	GCATTCTGCACCTGCAGATCC
Ing3-floxed-Forward	TAGCAGCCATCCACTGAGG
Ing3-floxed-Reverse	GTTACGGCAATCAGAGCTGC
Ing3-genomic-Reverse	CAGGAAGCTCTAAACCAGTGC
Cre-Forward	CATTTCTGGGGATTGCTTATAACAC
Cre-Reverse	TATTGAAACTCCAGCGCGGGCC

Table 2: PCR cycling conditions.

Program 1			**Program 2**			**Program 3**		
Temp. (°C)	Time (s)	Cycles	Temp. (°C)	Time (s)	Cycles	Temp. (°C)	Time (s)	Cycles
94	120	1 ×	95	120	1 ×	94	120	1 ×
94	15	35 ×	95	30	35 ×	94	15	35 ×
61	20		62	30		61	20	
68	30		68	30		68	60	
68	120	1 ×	68	300	1 ×	68	120	1 ×
18	∞	1 ×	18	∞	1 ×	18	∞	1 ×

Temp.: temperature

For PCR genotyping, the obtained DNA sample was used adhering to a One*Taq*® Quick-Load® protocol (catalogue number: M0486L; New England Biolabs, Frankfurt, Germany) modified for a total reaction volume of 15 µl. PCR was performed using the peqSTAR 96X Universal thermal cycler (catalogue number: PEQL95-05002-GBO; VWR International). Details regarding master mix preparation and reagents used are provided in Tables 3 and 4, respectively. DNA fragment separation was carried out by electrophoresis on a 1.5% agarose gel.

Table 3: Master mix for PB-CRE4 and CAG-Ing3-P2A-eGFP PCR.

Component	Volume per reaction (µl)	Stock concentration	Final concentration
One*Taq*® Quick-Load® 2 × Master Mix with Standard Buffer	7.5	2 ×	1 ×
Forward primer	0.5	10 µM	0.33 µM
Reverse primer	0.5	10 µM	0.33 µM
H_2O	6	-	-
Template DNA	0.5	-	-
Total volume	**15**		

Table 4: Master mix for *Ing3*-tm1c and *Ing3*-tm1d PCR.

Component	Volume per reaction (µl)	Stock concentration	Final concentration
One *Taq*® Quick-Load® 2 × Master Mix with Standard Buffer	7.5	2 ×	1 ×
Forward primer	0.375	10 µM	0.25 µM
Reverse primer	0.375	10 µM	0.25 µM
H_2O	6.25	-	-
Template DNA	0.5	-	-
Total volume	**15**		

2.6 Digital PCR

The concentration of extracted DNA was measured spectrophotometrically on the Eppendorf BioPhotometer® (Eppendorf, Hamburg, Germany) equipped with an Implen LabelGuard™ Microliter Cell (Implen, Munich, Germany). 80 ng template DNA was applied per dPCR chip to

fit into the narrow dynamic range of 200–2,000 copies per microlitre of final reaction (QuantStudio™ 3D Digital PCR System User Guide; Applied Biosystems™, division of Thermo Fisher Scientific, Waltham, Massachusetts, USA).

Primers and the probe targeting the undisrupted locus of *Ing3*, either wildtype or tm1c allele, respectively, were designed using the Primer Express™ software (version 2.0; Applied Biosystems™). The melting temperatures and secondary structures of the primers were predicted with the software tool NetPrimer (Premier Biosoft, San Francisco, California, USA). The amplicon secondary structure folding was evaluated on the Mfold Web Server (Zuker 2003). NCBI Primer-BLAST (Ye et al. 2012) was used to confirm the target specificity of the primers. Primers and the FAM™-labelled, ZEN™/Iowa Black® FQ double-quenched hydrolysis probe of the *Ing3* assay were synthesised at Integrated DNA Technologies (DNA Oligo and PrimeTime® Eco qPCR Probe, respectively; Leuven, Belgium).

The gene of interest was normalised to the single-copy nuclear gene *B2m* used before in a similar set-up of duplex dPCR (Hu 2019). The primers for *B2m* were ordered from Sigma-Aldrich (Standard, desalted DNA oligonucleotides). For copy number counting of *B2m*, a HydrolEasy™ probe was provided by PentaBase (Odense, Denmark). The probe was labelled with the reporter dye PentaYellow and the BHQ®-1 quencher at its 5' and 3' ends, respectively, and contained five proprietary pentabases. Table 5 lists primer and probe sequences in addition to corresponding amplicon lengths.

Table 5: Primers and probes for dPCR experiments.

Target gene	Primer/probe designation	Primer sequence (5'–3')	Amplicon length (bp)
Ing3	Ing3-Forward	CATTGGGACCCTCTAGGAGAGAT	82
	Ing3-Reverse	GCCCCCAAGTCCCTCATAA	
	In3-Probe	/56-FAM/TTACGTAGA/ZEN/TACCT GGATATGGAGTGAGGGCA/3IABkFQ/	
B2m	B2m-Forward	CTCAGAAACCCCTCAAATTCAAGTA	96
	B2m-Reverse	GGCGGGTGGAACTGTGTTAC	
	B2m-Probe	/PentaYellow/CTCACGCCACCCAC CGGAGAATG/BHQ-1/	

dPCR was performed on the QuantStudio™ 3D Digital PCR System (Applied Biosystems™). The master mix (catalogue number: A26358; Applied Biosystems™) was composed as

outlined in Table 6. The automated chip loader (catalogue number: 4482592; Applied Biosystems™) was used to load 14.5 µl of the reaction mix onto the silicon chip (catalogue number: A26316; Applied Biosystems™). The chip, encompassing 20,000 reaction wells each with a capacity of 755 pl, was manually covered with immersion fluid and sealed with the provided lid according to manufacturer's instruction. Amplification was performed on a tilted flat block thermal cycler (GeneAmp® PCR System 9700; Applied Biosystems™) (Table 7). End-point signals were read by the QuantStudio™ 3D Digital PCR Instrument (catalogue number: 4481097; Applied Biosystems™) and curated on the QuantStudio™ 3D AnalysisSuite™ Cloud Software (version 3.1.6-PRC-build2; Applied Biosystems™).

Table 6: Master mix for dPCR.

Component	Volume per reaction (µl)	Stock concentration	Final concentration
QuantStudio™ 3D Digital PCR Master Mix v2	9.00	2 ×	1 ×
Ing3-Forward	0.36	10 µM	0.2 µM
Ing3-Reverse	0.36	10 µM	0.2 µM
Ing3-Probe	0.36	10 µM	0.2 µM
B2m-Forward	0.36	10 µM	0.2 µM
B2m-Reverse	0.36	10 µM	0.2 µM
B2m-Probe	0.36	10 µM	0.2 µM
H_2O	1.84	-	-
Template DNA	5.00	-	-
Total volume	**18.00**		

Table 7: dPCR cycling conditions.

Temperature (°C)	Time	Cycles
96	10 min	1 ×
98	30 s	45 ×
60	2 min	
60	2 min	1 ×
10	∞	1 ×

Subsequent statistical analysis including mean and standard deviation calculation as well as plotting the results was performed with the Microsoft Excel software (version 16.0.12527.20260; Microsoft Corporation, Redmond, Washington, USA).

2.7 Immunohistochemical staining

Paraffin blocks were cut into 5 µm sections (HM 325 Rotary Microtome; Thermo Scientific™), paraffin ribbons were placed in a water bath at 37 °C and mounted onto adhesive-coated slides (catalogue number: 48311-703; VWR International). After air-drying overnight at room temperature, tissues were deparaffinized by two rounds of incubation in xylene for 15 minutes. Rehydration was performed in consecutive baths of 100% ethanol, again 100% ethanol in a different vessel, 95% ethanol, 70% ethanol and double distilled water (ddH_2O) for two minutes each.

Slides were fully submerged in antigen retrieval buffer (5 ml of Rodent Decloaker (catalogue number: RD913; Biocare Medical, Concord, California, USA) to 45 ml of ddH_2O) and the buffer was brought to a boil in a microwave and then heated at 95 °C for another 20 minutes. After cooling down, the samples were washed with Tris-buffered saline with Tween 20 (TBST) washing buffer (150 mM NaCl, 20 mM Tris, pH 7.6 supplemented with 0.1% Tween 20) four times for four minutes and then incubated with Dako REAL™ Peroxidase-Blocking Solution (catalogue number: S202386-2; Dako, division of Agilent Technologies, Santa Clara, California, USA) for five minutes. Following another washing step (four times for four minutes with TBST), sections were treated with blocking solution (TBST supplemented with 2% BSA) for 30 minutes at room temperature. Samples were washed once for two minutes with TBST and then incubated with primary anti-ING3 monoclonal antibody clone 2A2 (in-house, Riabowol Laboratory, University of Calgary) at different dilutions (1:50, 1:100 and 1:200, respectively; in 150 mM NaCl, 20 mM Tris, pH 7.6 supplemented with 1% BSA) overnight at 4 °C. Designated negative controls were treated with TBST instead of primary antibody. After primary antibody removal by four consecutive washes with TBST for four minutes each, sections were incubated with horseradish peroxidase (HRP)-labelled polymer anti-mouse reagent (catalogue number: K4000; Dako) for 30 minutes at room temperature. After washing four times in TBST for four minutes each, sections were treated with 3,3'-Diaminobenzidine (DAB) reagent (catalogue number: K3468; Dako; 1 ml DAB substrate supplemented with one drop of DAB chromogen) and incubated for approximately two minutes until a visible change of colour occurred. Samples were washed with ddH_2O and then counterstained with

hematoxylin (catalogue number: GHS232; Sigma-Aldrich) for five minutes. Slides were rinsed with warm tap water (approximately 37 °C) for three minutes, submerged in TBST for one minute and washed with warm ddH_2O for one minute.

Dehydration was performed by dipping slides 15 times per vessel in a graded series of alcohol (70%, 95%, two different vessels containing 100% ethanol) and finally two different vessels filled with xylene. Mounting solution (catalogue number: EM897L; Biocare Medical) was applied and a coverslip was placed on the specimen.

Staining success was confirmed through brightfield microscopy (CX41 Upright Microscope; Olympus, Tokyo, Japan). Images were acquired with QCapture™ (software version 18.3; Teledyne QImaging, Surrey, Canada) in combination with a digital camera (Q-Color5™ Digital Imaging System; Olympus) and edited using the GIMP software (version 2.10.18).

3 Results

3.1 Animal breeding

Concerning the prostate-specific *Ing3* knockout, breeding efforts summarized in Figure 2A resulted in the generation of 17 mice. Five mice (29–36 weeks of age) were included in the dPCR analysis and one mouse (35 weeks of age) was subjected to immunohistochemical staining against ING3. No abnormalities with regard to prostate size and gross anatomy were found.

Adhering to the breeding scheme depicted in Figure 2B, a total number of 19 ubiquitous *Ing3* knockout mice were obtained, with the ratio of female to male individuals being 12:7. Consistent with the experimental data reported by Fink and colleagues (Fink et al. 2020), all of those animals harboured the CAG-Ing3-P2A-eGFP transgenic construct, driving ectopic ING3 expression, and thus rescuing the embryonic lethal phenotype of *Ing3* depleted mice. Four individuals were randomly selected and enrolled into the dPCR calibration experiment.

Genotypes were determined by means of conventional PCR. A comprehensive list of all animals included in the experiments can be found in the supplementary data (Tables S1, S2 and S3).

3.2 Digital PCR calibration and recombination efficiency assessment

All DNA samples included in the dPCR calibration were obtained from ear biopsies from ubiquitous *Ing3* knockout animals ($Ing3^{\Delta/\Delta}$), from heterozygous carriers of the *Ing3*-tm1d allele ($Ing3^{+/\Delta}$) and homozygous *Ing3*-tm1c mice ($Ing3^{fl/fl}$).

The assay configuration with regard to the primer annealing sites does not allow for a distinction between *Ing3*-tm1c and wildtype *Ing3* alleles (Figure 3A). The overall outcome of the calibration is provided as a bar chart in Figure 3B, with the ratio of the concentrations of the two targets (1 - (*Ing3*/*B2m*)) being plotted on the y-axis for the three distinct genotypes of *Ing3* (fl/fl: -1.65% ± 1.49 percentage points, n=4; +/∆: 49.07% ± 1.47 percentage points, n=6; ∆/∆: 99.90% ± 0.13 percentage points, n=4). Values of 0% indicate that the copy number of undisrupted *Ing3* is equal to the copy count of *B2m* in the biological sample, whereas outputs of 50% and 100% point towards *B2m* being twice as abundant compared to *Ing3* and a total lack of *Ing3*, respectively. Values below 0% can be attributed to method-inherent fluctuations of measurements.

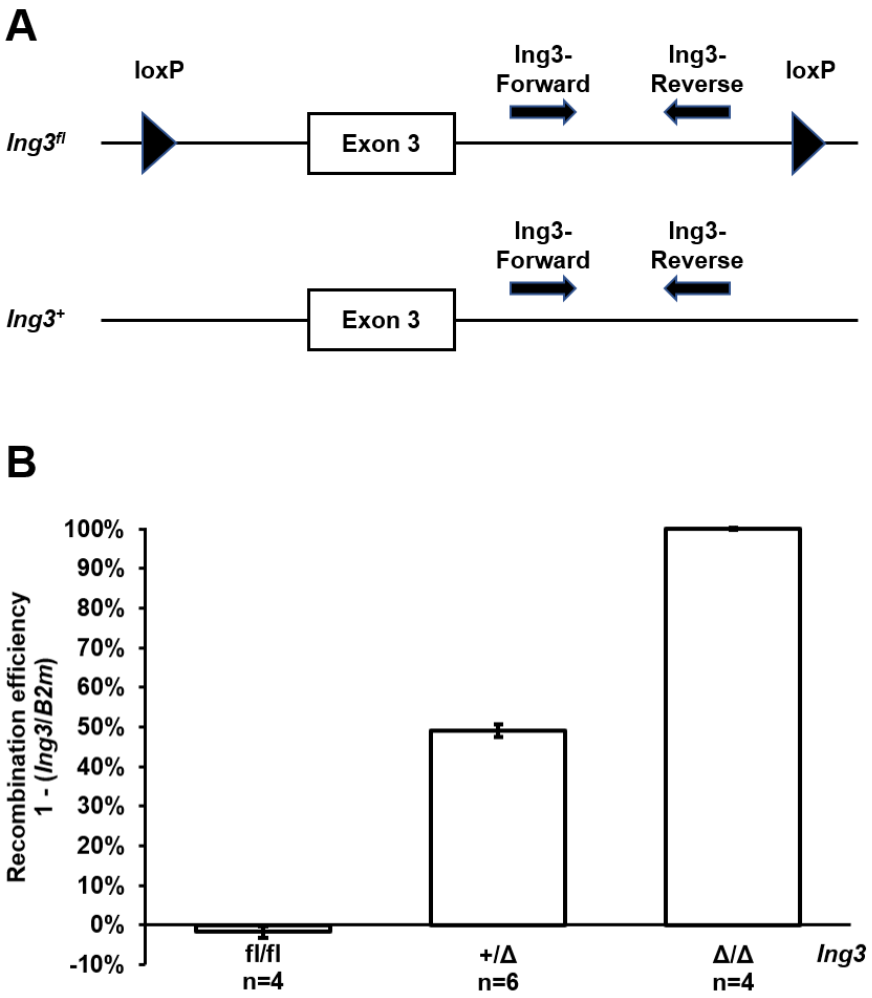

Figure 3. dPCR calibration: target sequences and outcome. (A) Representation of targeted *Ing3* alleles. Given that the primer annealing sites (arrows) are located between the loxP sequences, the *Ing3*$^{\Delta}$ allele is not detected and distinguishing between the *Ing3*^{fl} and *Ing3*$^{+}$ allele is not feasible. **(B)** The ratio of the concentrations of the two targets (1 - (*Ing3*/*B2m*)) is depicted for the following *Ing3* genotypes: *Ing3*$^{fl/fl}$, *Ing3*$^{+/\Delta}$ and *Ing3*$^{\Delta/\Delta}$. The standard deviation is indicated by error bars. Sample numbers are indicated below the bars.

To evaluate Cre-mediated recombination in the prostate-specific knockout (*Ing3*$^{fl/fl}$; PbCre4$^{+/T}$), DNA samples derived from anterior, dorsolateral and ventral prostatic lobes were subjected to the established dPCR assay (anterior lobe: 23.05% ± 9.10 percentage points, n=5; dorsolateral lobe: 25.06% ± 3.76 percentage points, n=5; ventral lobe: 23.32% ± 3.99 percentage points, n=3). In addition, age-matched *Ing3*-tm1c mice lacking the PB-Cre4 transgene (*Ing3*$^{fl/fl}$; PbCre4$^{+/+}$) were incorporated as controls (anterior lobe: 0.35% ± 1.84 percentage points, n=5; dorsolateral lobe: 0.62% ± 2.73 percentage points, n=5; ventral lobe: -3.37% ± 2.53 percentage

points, n=4). There appears to be no significant difference in the Cre-mediated recombination efficiency between the distinct prostate lobes (Figure 4).

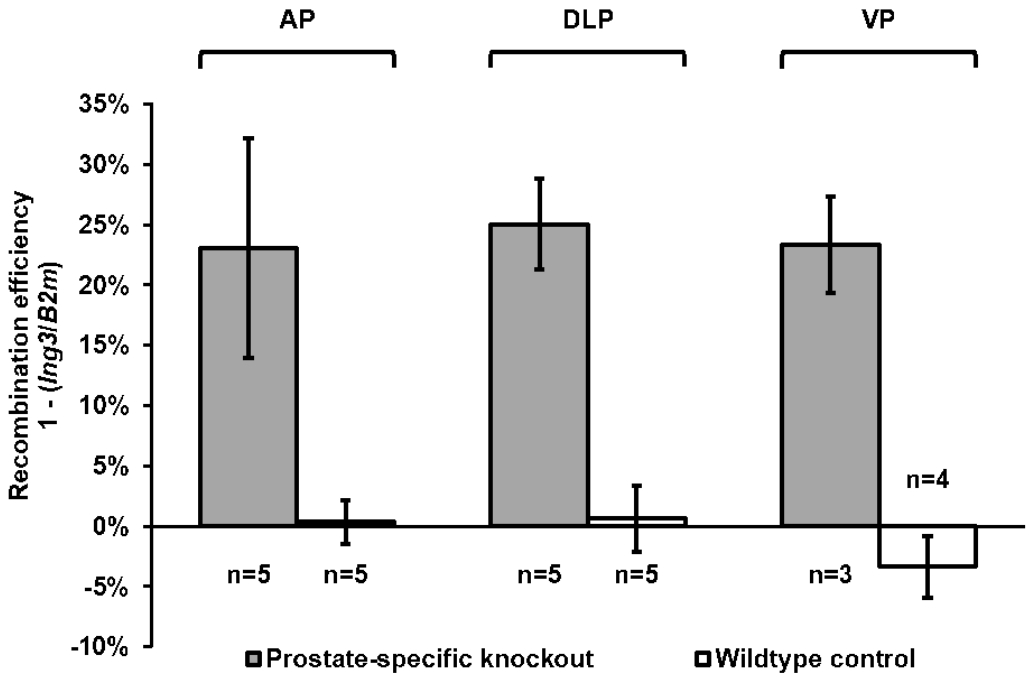

Figure 4. Determination of recombination efficiency in the prostate-specific *Ing3* knockout by dPCR. While recombination events did occur in PB-Cre4 positive homozygous *Ing3*-tm1c mice, there appears to be no major difference in the recombination efficiency between the prostatic lobes. In homozygous *Ing3*-tm1c mice lacking the PB-Cre4 transgene no recombination events were detected. The standard deviation is indicated by error bars. Sample numbers are indicated below the bars. (AP: anterior prostatic lobe, DLP: dorsolateral prostatic lobe, VP: ventral prostatic lobe)

Instrument readouts including Poisson distribution parameters and quality assessment metrics are provided in the supplementary data (Tables S4 and S5) in compliance with the “Minimum Information for Publication of Quantitative Digital PCR Experiments” guidelines (Huggett et al. 2013). Samples that did not fit into the dynamic range of 200–2,000 copies per microlitre were omitted from statistical analysis (highlighted in grey).

3.3 ING3 staining of murine tissues

To gain insights into murine ING3 expression at the protein level, four tissues sampled from male wildtype mice based on a previous *Ing3-LacZ* reporter mouse study on ING3 expression

(Barones et al., manuscript in preparation) were subjected to IHC staining against ING3. The most suitable primary antibody dilution for optimal signal-to-noise ratio was determined to be 1:100. Proximal and distal tubules in the renal cortex displayed high ING3 levels (Figure 5A), whereas weak diffuse staining was noted in liver and cerebrum sections (Figure 5B and 5C). A ganglion randomly encountered within periprostatic soft tissue of a PB-Cre4 negative homozygous *Ing3*-tm1c mouse exhibited moderate staining (Figure 5D).

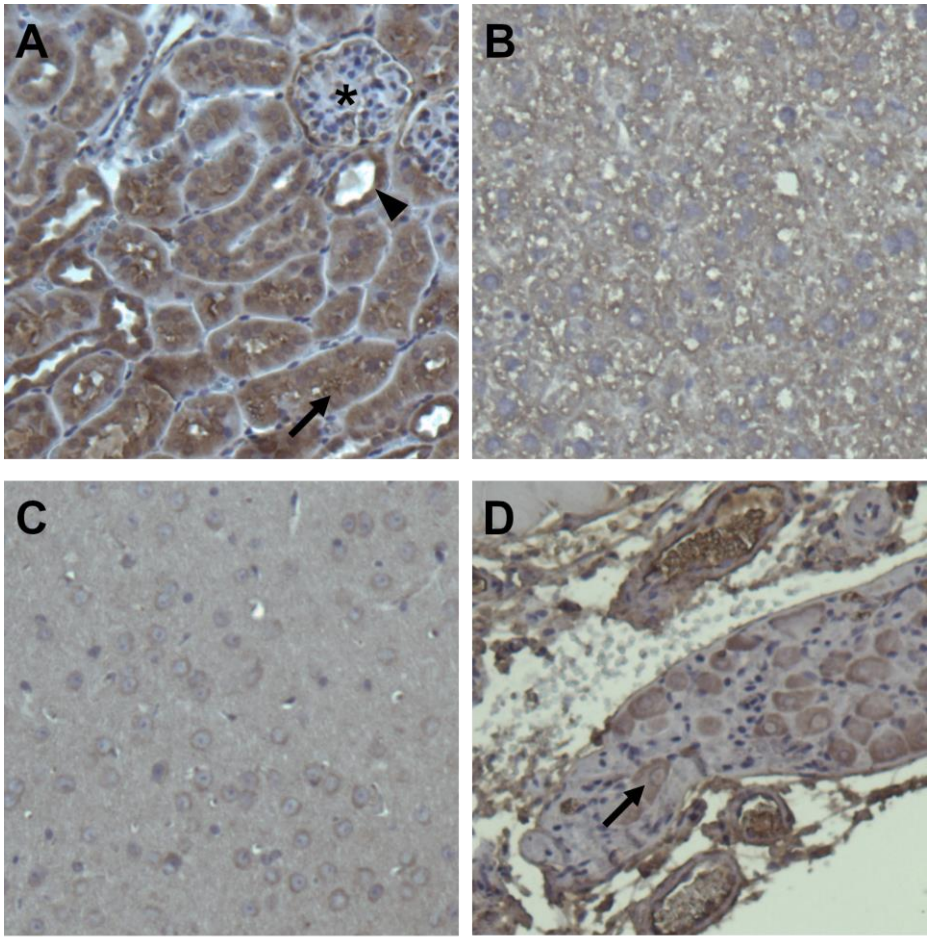

Figure 5. Representative images of ING3 staining in various murine tissues. (A) Strong staining in proximal (arrow) and distal (arrowhead) tubules of the renal cortex. A glomerulus is highlighted (asterisk). Weak diffuse staining in **(B)** liver and **(C)** cerebrum sections. **(D)** Moderate staining intensity in neuron cell body (arrow) of a ganglion in periprostatic soft tissue. Kidney, liver and cerebrum were extracted from a male wildtype mouse (n=1), whereas prostate tissue was harvested from a PB-Cre4 negative homozygous *Ing3*-tm1c mouse (n=1). Magnification 200 ×.

For recombination efficiency assessment in the prostate-specific knockout model, ING3 staining in the anterior and dorsolateral prostatic lobes of a PB-Cre4 positive homozygous

Ing3-tm1c mouse (Figure 6A and 6B) was compared to a PB-Cre4 negative control mouse (Figure 6C and 6D) with otherwise identical genetic background. Overall staining intensity was very faint, and thus it was not feasible to draw qualitative or quantitative conclusions on the recombination efficiency based on IHC staining. In sections where the primary antibody was omitted, no ING3 staining signal was detected (Figure 6E and 6F).

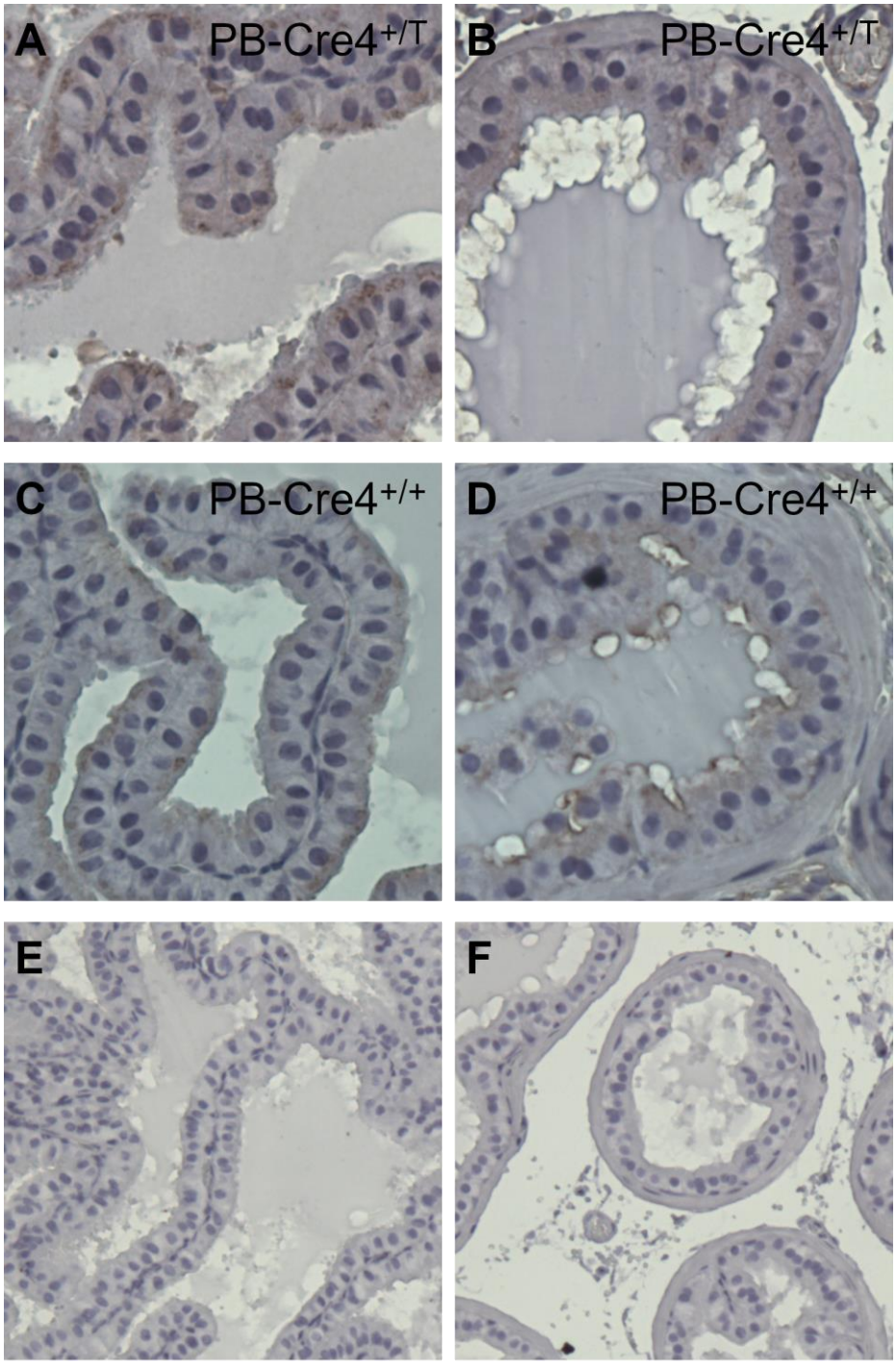

Figure 6. Representative images of ING3 staining in murine anterior and dorsolateral prostatic lobes. (A) Anterior and **(B)** dorsolateral prostate of a PB-Cre4 positive homozygous *Ing3*-tm1c mouse. **(C)** Anterior and **(D)** dorsolateral prostate of a PB-Cre4 negative homozygous *Ing3*-tm1c mouse. Panels **(E)** and **(F)** display sections of anterior and dorsolateral prostatic lobes, respectively, of a PB-Cre4 positive homozygous *Ing3*-tm1c mouse where primary antibody was omitted. Magnification 400 × (A, B, C and D) and 200 × (E and F).

4 Discussion

Paternal transmission of PB-Cre4 enforces tissue-specific Cre-mediated recombination in the epithelial lining of the prostatic glands (Wu et al. 2001). Considering the fact that wildtype mice are not prone to neoplastic disorders of the prostate, any abnormalities observed in genetically engineered mice most likely stem from the genetic manipulation (Shappell et al. 2004). Interestingly, upon gross anatomical inspection of 17 prostate-specific *Ing3* knockouts aged from 10–85 weeks, there was no evidence of prostate tumourigenesis. In contrast, deletion of the classical tumour suppressor gene phosphatase and tensin homolog (*Pten*), which dephosphorylates phosphatidylinositol-(3,4,5)-trisphosphate and acts as a negative regulator of the protein kinase B signalling pathway, leads to invasive adenocarcinoma with a reported cumulative incidence of 100% within 29 weeks of age (Wang et al. 2003). The same tissue-specific Cre deleter mouse line was used in this thesis. Therefore, I postulate that *Ing3* must not be regarded as a classical tumour suppressor gene in the context of prostate cancer development, since no changes in growth and size were observed.

Although most studies report the assumption that *Ing3* acts as a negative regulator of cell growth and proliferation, hence the name inhibitor of growth 3, overexpression of ING3 has recently been implicated with enhanced cellular proliferation in *ex vivo* prostate tissue cultures (McClurg et al. 2018). Further experiments focused at investigating the oncogenic potential of *Ing3* are necessary. Therefore, a double knockout of *Ing3* and *Pten* or a triple knockout including *p53* (Martin et al. 2011) might be required for neoplastic proliferation and development of metastases of the prostate.

dPCR analysis aimed to detect and measure recombination events in the prostate tissue of the conditional *Ing3* knockout. As opposed to conventional quantitative PCR, dPCR facilitates highly accurate absolute quantification of nucleic acid sequences and does not rely on a standard curve (Huggett et al. 2013). Taken together, it is a versatile and convenient tool to quantitatively evaluate genetic alterations in transgenic mice.

To set up a control for 50% and 100% recombination events (Figure 3) and to confirm the lethal phenotype of a homozygous mutant *Ing3* strain described in (Fink et al. 2020), female transgenic PB-Cre4 mice were successfully used to create a ubiquitous *Ing3* knockout based on the Cre-loxP system. No homozygous *Ing3* knockout mice were born, implicating that *Ing3* exerts vital biological functions during embryogenesis. A viable phenotype was restored by

ectopic overexpression of ING3 through introduction of the CAG-Ing3-P2A-eGFP transgenic construct.

Although it has been reported that the epithelial activity of Cre varies between the anterior, dorsolateral and ventral prostate lobes when the PB-Cre4 strain was crossed to an inducible *lacZ* reporter strain (Wu et al. 2001), dPCR did not uncover a major difference in the recombination efficiency between those distinct anatomical structures (Figure 4). However, Cre activity is likely to be influenced by several factors, such as target chromatin accessibility and genomic context of the target sequence. Since the underlying recombination events are cumulative and cannot be reversed, the subject's age must also be taken into consideration when evaluating recombination frequencies.

It is important to note that the dissected prostate samples the DNA templates were derived from, consist not only of epithelial parenchymal cells but also of stroma, including a fibromuscular tunica surrounding the glands, loose interlobular connective tissue, blood vessels and nerves. Within the epithelial layer, differentiated secretory cells, basal cells and neuroendocrine cells can be distinguished (Oliveira et al. 2016). Claiming that the epithelial recombination efficiency does not vary between the anterior, dorsolateral and ventral prostate lobes is valid only if the distinct lobes exhibit the same ratio of parenchymal to stromal cells and a uniform recombination pattern in the stromal cells. To address the recombination efficiency in isolated cell populations of the prostate, for instance the secretory cells, one would need to deploy reliable and reproducible cell separation methods prior to DNA extraction.

On another note, the question needs to be raised whether cellular Cre activity in homozygous tm1c mice always results in the deletion of both floxed alleles. In order to bypass this issue, it might be beneficial to generate compound heterozygotes, by crossing *Ing3*-tm1c mice to an insertional mutant of *Ing3* transgenic line, designated as B6(Cg)-Tyr^{c-2J} Tg(UBC-mCherry)1Phbs/J (JAX stock number 017614; Fink et al. 2020), and re-evaluate the prostate-specific recombination efficiency in mice bearing the PB-Cre4 transgene. In this way, only one floxed allele of *Ing3* needs to be recombined per cell, while the other allele is already disrupted. Nevertheless, with the described dPCR assay I have established a framework that might be useful for the molecular characterisation of future conditional knockout models.

IHC staining for ING3 in prostate tissues of the conditional *Ing3* knockout mouse using the 2A2 anti-ING3 monoclonal antibody did not meet the expectations of reflecting the results of the dPCR analysis. Compared to other murine tissues, the prostate exhibited faint staining pointing

towards low expression of ING3 (as seen in Figure 5 and 6). Due to the poor signal-to-noise ratio, it was not feasible to estimate the recombination frequency in the prostate epithelium, highlighting the need for more sensitive and reliable immunological methods.

5 Summary

The inhibitor of growth, family member 3 (ING3) acts as an epigenetic reader and, through physical interactions with histone modifying enzymes and subsequent chromatin remodelling processes, is involved in various cellular functions, such as cell cycle control, cell growth and apoptosis. Although ING3 has been assigned a tumour suppressor candidate status in many types of cancers, its role in the initiation and progression of prostate cancer remains to be elucidated. The aim of this thesis was to establish a murine prostate-specific and ubiquitous *Ing3* knockout model based on Cre-mediated excision of a loxP flanked critical exon and assess the recombination efficiency in the prostatic glands at the DNA and protein level.

Paternal inheritance of the PB-Cre4 construct was used to generate the prostate-specific *Ing3* knockout, while for the generation of the ubiquitous knockout, a female mouse harbouring the PB-Cre4 transgene was utilised as a global deleter. A duplex probe-based digital PCR assay capable of counting undisrupted *Ing3* copies was designed, and the impact of DNA recombination on the protein level was investigated by immunohistochemical staining for ING3 in prostate tissue samples.

Consistent with a recent study, no homozygous ubiquitous *Ing3* knockout mice were born, unless ING3 expression was restored by breeding with a transgenic mouse bearing the CAG-Ing3-P2A-eGFP construct. In the prostate-specific knockout, digital PCR analysis revealed mosaic gene deletion. Similar recombination efficiencies in the anterior, ventral and dorsolateral prostate lobes at approximately 25% in epithelial and mesenchymal cells together were achieved. ING3 staining in the anterior and dorsolateral prostate was very faint, and no differences in signal intensity between a knockout specimen and wildtype control were detected. Upon dissection, no animal displayed gross anatomical abnormalities that I could link to prostate cancer development.

This thesis provides evidence that *Ing3* behaves differently from classical tumour suppressors, like *Pten*, where invasive adenocarcinoma is observed in a comparable Cre-dependent knockout model. Furthermore, I confirmed the embryonic lethal phenotype of the *Ing3* depleted homozygous mice. While digital PCR is a versatile, convenient and highly accurate tool for the detection and absolute quantification of the genetic alterations in this model, recombination efficiency assessment based on immunohistochemistry was not feasible due to a poor signal-to-noise ratio.

6 Zusammenfassung

Das „Inhibitor of Growth 3“ (*ING3*)-Gen codiert für ein Protein, welches spezifische epigenetische Markierungen erkennt und über Interaktionen mit Histon-modifizierenden Enzymen dynamische Veränderungen der Chromatinstruktur vermittelt. Es beeinflusst zahlreiche biologische Prozesse, wie Zellwachstum, Zellzykluskontrolle und Apoptose. *ING3* fungiert in mehreren Krebsarten als Tumorsuppressorgen-Kandidat, allerdings ist seine Rolle in der Entwicklung des Prostatakarzinoms weitgehend unerforscht. Ziel der Arbeit war die Etablierung einer auf dem Cre-loxP-Rekombinationssystem beruhenden prostataspezifischen und ubiquitären *Ing3*-Knockout-Mauslinie. Darüber hinaus sollte in der gewebsspezifischen Linie die Rekombinationseffizienz auf DNA- und Proteinebene untersucht werden.

Für die Generierung des ubiquitären Knockouts wurde ein weiblicher Träger des PB-Cre4 Transgens als „Cre-deleter“ herangezogen. Paternale Vererbung des PB-Cre4 Konstruktes diente der Erzeugung des prostataspezifischen Knockouts. Eine sondenbasierte duplex-digitale PCR, welche die absolute Quantifizierung funktionaler *Ing3*-Kopien erlaubt, wurde konzipiert. Zusätzlich wurde mittels Immunhistochemie die Verteilung von ING3 in Prostataschnitten untersucht.

Im Einklang mit einer kürzlich veröffentlichten Studie war die homozygote *Ing3*-Deletion im Embryonalstadium letal und ein lebensfähiger Phänotyp konnte nur durch Verpaarung mit der CAG-Ing3-P2A-eGFP-Linie gezüchtet werden. In der prostataspezifischen Knockout-Linie zeigte die digitale PCR den Erfolg der unvollständigen genetischen Rekombination und den daraus resultierenden Mosaizismus. Die Rekombinationseffizienzen zwischen den anterioren, dorsolateralen und ventralen Prostatalappen unterschieden sich nicht. Die immunhistochemische Färbung von ING3 in der anterioren und dorsolateralen Prostata war schwach, zudem konnten keine Unterschiede in der Signalintensität zwischen einer Knockout-Maus und einer Wildtyp-Kontrolle detektiert werden. Bei der Tiersektion wurden keine makroskopischen Hinweise auf eine Entartung der Prostata gefunden.

Diese Arbeit bestätigt den embryonal letalen Phänotyp der homozygoten *Ing3*-Knockout-Maus. Darüber hinaus wurde die Annahme gestärkt, wonach sich *Ing3* nicht im Sinne eines klassischen Tumorsuppressors, wie beispielsweise *Pten*, verhält. Die digitale PCR erwies sich als vielseitige, zweckdienliche und hochakkurate Methode für die Evaluierung der genetischen Veränderung in dem beschriebenen Tiermodell. Dagegen ließ die Immunhistochemie keine zufriedenstellenden Schlüsse auf die Rekombinationseffizienz zu.

7 List of abbreviations

AR	Androgen receptor
Cre	Cyclization recombinase
DAB	3,3'-Diaminobenzidine
ddH_2O	Double distilled water
dPCR	Digital PCR
FLP	Flippase
FRT	Flippase recognition target
HAT	Histone acetyltransferase
HRP	Horseradish peroxidase
IHC	Immunohistochemistry
ING3	Inhibitor of growth family member 3 (human gene)
Ing3	Inhibitor of growth family member 3 (mouse gene)
ING3	Inhibitor of growth protein 3 (human or mouse protein)
lacZ	Beta-galactosidase gene
loxP	Locus of crossover in P1
neo	Neomycin resistance gene
NuA4	Nucleosome acetyltransferase of histone H4
PHD	Plant homeodomain
Pten	Phosphatase and tensin homolog (mouse gene)
TBST	Tris-buffered saline with Tween 20

8 References

Almami A, Hegazy SA, Nabbi A, Alshalalfa M, Salman A, Abou-Ouf H, Riabowol K, Bismar TA. 2016. ING3 is associated with increased cell invasion and lethal outcome in ERG-negative prostate cancer patients. Tumor Biology, 37(7):9731–9738.

Berger SL. 2007. The complex language of chromatin regulation during transcription. Nature, 447(7143):407–412.

Birbach A. 2013. Use of PB-Cre4 mice for mosaic gene deletion. PloS One, 8(1):e53501.

Broach JR, Guarascio VR, Jayaram M. 1982. Recombination within the yeast plasmid 2mu circle is site-specific. Cell, 29(1):227–234.

Coons AH, Creech HJ, Jones RN. 1941. Immunological properties of an antibody containing a fluorescent group. Proceedings of the Society for Experimental Biology and Medicine, 47(2):200–202.

Doyon Y, Selleck W, Lane WS, Tan S, Cote J. 2004. Structural and functional conservation of the NuA4 histone acetyltransferase complex from yeast to humans. Molecular and Cellular Biology, 24(5):1884–1896.

Fink D, Yau T, Nabbi A, Wagner B, Wagner C, Hu SM, Lang V, Handschuh S, Riabowol K, Rulicke T. 2020. Loss of Ing3 Expression Results in Growth Retardation and Embryonic Death. Cancers, 12(1).

Garkavtsev I, Kazarov A, Gudkov A, Riabowol K. 1996. Suppression of the novel growth inhibitor p33ING1 promotes neoplastic transformation. Nature Genetics, 14(4):415–420.

Gunduz M, Ouchida M, Fukushima K, Ito S, Jitsumori Y, Nakashima T, Nagai N, Nishizaki K, Shimizu K. 2002. Allelic loss and reduced expression of the ING3, a candidate tumor suppressor gene at 7q31, in human head and neck cancers. Oncogene, 21(28):4462–4470.

He GHY, Helbing CC, Wagner MJ, Sensen CW, Riabowol K. 2005. Phylogenetic analysis of the ING family of PHD finger proteins. Molecular Biology and Evolution, 22(1):104–116.

Hu SM. 2019. Analysis of Fluorescently Labelled Cre/loxP Inducible Ing3 Transgenic Mice. [Bachelor thesis]. Vienna: University of Veterinary Medicine.

Huggett JF, Foy CA, Benes V, Emslie K, Garson JA, Haynes R, Hellemans J, Kubista M, Mueller RD, Nolan T, et al. 2013. The digital MIQE guidelines: Minimum Information for Publication of Quantitative Digital PCR Experiments. Clinical Chemistry, 59(6):892–902.

Kataoka H, Bonnefin P, Vieyra D, Feng X, Hara Y, Miura Y, Joh T, Nakabayashi H, Vaziri H, Harris CC, et al. 2003. ING1 represses transcription by direct DNA binding and through effects on p53. Cancer Research, 63(18):5785–5792.

Kitahara J, Chiba N, Sakamoto H, Nakagawa Y. 2003. Alteration of gene expressions by the overexpression of mitochondrial phospholipid hydroperoxide glutathione peroxidase (mtPHGPx). Gene Expression, 11(2):77–83.

Liang G, Lin JCY, Wei V, Yoo C, Cheng JC, Nguyen CT, Weisenberger DJ, Egger G, Takai D, Gonzales FA, et al. 2004. Distinct localization of histone H3 acetylation and H3-K4 methylation to the transcription start sites in the human genome. Proceedings of the National Academy of Sciences of the United States of America, 101(19):7357–7362.

Lu M, Chen F, Wang Q, Wang K, Pan Q, Zhang X. 2012. Downregulation of inhibitor of growth 3 is correlated with tumorigenesis and progression of hepatocellular carcinoma. Oncology Letters, 4(1):47–52.

Mahler Convenor M, Berard M, Feinstein R, Gallagher A, Illgen-Wilcke B, Pritchett-Corning K, Raspa M. 2014. FELASA recommendations for the health monitoring of mouse, rat, hamster, guinea pig and rabbit colonies in breeding and experimental units. Laboratory Animals, 48(3):178–192.

Martin P, Liu Y-N, Pierce R, Abou-Kheir W, Casey O, Seng V, Camacho D, Simpson RM, Kelly K. 2011. Prostate epithelial Pten/TP53 loss leads to transformation of multipotential progenitors and epithelial to mesenchymal transition. The American Journal of Pathology, 179(1):422–435.

McClurg UL, Nabbi A, Ricordel C, Korolchuk S, McCracken S, Heer R, Wilson L, Butler LM, Irving-Hooper BK, Pedeux R, et al. 2018. Human ex vivo prostate tissue model system identifies ING3 as an oncoprotein. British Journal of Cancer, 118(5):713–726.

Nabbi A, Almami A, Thakur S, Suzuki K, Boland D, Bismar TA, Riabowol K. 2015. ING3 protein expression profiling in normal human tissues suggest its role in cellular growth and self-renewal. European Journal of Cell Biology, 94(5):214–222.

Nabbi A, McClurg UL, Thalappilly S, Almami A, Mobahat M, Bismar TA, Binda O, Riabowol KT. 2017. ING3 promotes prostate cancer growth by activating the androgen receptor. BMC Medicine, 15(1):103.

Nagashima M, Shiseki M, Miura K, Hagiwara K, Linke SP, Pedeux R, Wang XW, Yokota J, Riabowol K, Harris CC. 2001. DNA damage-inducible gene p33ING2 negatively regulates cell proliferation through acetylation of p53. Proceedings of the National Academy of Sciences of the United States of America, 98(17):9671–9676.

Nagashima M, Shiseki M, Pedeux RM, Okamura S, Kitahama-Shiseki M, Miura K, Yokota J, Harris CC. 2003. A novel PHD-finger motif protein, p47ING3, modulates p53-mediated transcription, cell cycle control, and apoptosis. Oncogene, 22(3):343–350.

Oliveira DSM, Dzinic S, Bonfil AI, Saliganan AD, Sheng S, Bonfil RD. 2016. The mouse prostate: a basic anatomical and histological guideline. Bosnian Journal of Basic Medical Sciences, 16(1):8–13.

Shappell SB, Thomas G V, Roberts RL, Herbert R, Ittmann MM, Rubin MA, Humphrey PA, Sundberg JP, Rozengurt N, Barrios R, et al. 2004. Prostate pathology of genetically engineered mice: definitions and classification. The consensus report from the Bar Harbor meeting of the Mouse Models of Human Cancer Consortium Prostate Pathology Committee. Cancer Research, 64(6):2270–2305.

Shi X, Hong T, Walter KL, Ewalt M, Michishita E, Hung T, Carney D, Pena P, Lan F, Kaadige MR, et al. 2006. ING2 PHD domain links histone H3 lysine 4 methylation to active gene repression. Nature, 442(7098):96–99.

Shiseki M, Nagashima M, Pedeux RM, Kitahama-Shiseki M, Miura K, Okamura S, Onogi H, Higashimoto Y, Appella E, Yokota J, et al. 2003. p29ING4 and p28ING5 bind to p53 and p300, and enhance p53 activity. Cancer Research, 63(10):2373–2378.

Skarnes WC, Rosen B, West AP, Koutsourakis M, Bushell W, Iyer V, Mujica AO, Thomas M, Harrow J, Cox T, et al. 2011. A conditional knockout resource for the genome-wide study of mouse gene function. Nature, 474(7351):337–342.

Sternberg N, Hamilton D. 1981. Bacteriophage P1 site-specific recombination. I. Recombination between loxP sites. Journal of Molecular Biology, 150(4):467–486.

Sundberg SO, Wittwer CT, Gao C, Gale BK. 2010. Spinning disk platform for microfluidic digital polymerase chain reaction. Analytical Chemistry, 82(4):1546–1550.

Vogelstein B, Kinzler KW. 1999. Digital PCR. Proceedings of the National Academy of Sciences, 96(16):9236–9241.

Wang S, Gao J, Lei Q, Rozengurt N, Pritchard C, Jiao J, Thomas G V, Li G, Roy-Burman P, Nelson PS, et al. 2003. Prostate-specific deletion of the murine Pten tumor suppressor gene leads to metastatic prostate cancer. Cancer Cell, 4(3):209–221.

Wang Y, Li G. 2006. ING3 promotes UV-induced apoptosis via Fas/caspase-8 pathway in melanoma cells. The Journal of Biological Chemistry, 281(17):11887–11893.

Wang Y, Dai DL, Martinka M, Li G. 2007. Prognostic significance of nuclear ING3 expression in human cutaneous melanoma. Clinical Cancer Research, 13(14):4111–4116.

Wu X, Wu J, Huang J, Powell WC, Zhang J, Matusik RJ, Sangiorgi FO, Maxson RE, Sucov HM, Roy-Burman P. 2001. Generation of a prostate epithelial cell-specific Cre transgenic mouse model for tissue-specific gene ablation. Mechanisms of Development, 101(1–2):61–69.

Ye J, Coulouris G, Zaretskaya I, Cutcutache I, Rozen S, Madden TL. 2012. Primer-BLAST: a tool to design target-specific primers for polymerase chain reaction. BMC Bioinformatics, 13:134.

Zuker M. 2003. Mfold web server for nucleic acid folding and hybridization prediction. Nucleic Acids Research, 31(13):3406–3415.

9 List of figures and tables

10 Supplementary data

Table S1: Animals used for dPCR calibration.

Animal ID	Sex	*Ing3*
0117-0394	male	Δ/+
0120-0172	female	fl/fl
0120-0173	female	fl/fl
0120-0174	female	fl/fl
0120-0176	female	fl/fl
0149-0460	female	Δ/+
0149-0461	female	Δ/Δ
0149-0462	female	Δ/+
0149-0463	female	Δ/+
0149-0464	female	Δ/+
0149-0465	female	Δ/Δ
0149-0466	male	Δ/Δ
0149-0467	male	Δ/+
0149-0468	male	Δ/Δ

Table S2: Animals used for prostate-specific recombination efficiency assessment by dPCR.

Animal ID	Sex	*Ing3*	Pb-Cre4	Date of birth	Date of prostate harvest	Age (weeks)
0149-0417	male	fl/fl	+/+	05.06.2019	12.02.2020	36
0149-0418	male	fl/fl	+/T	05.06.2019	12.02.2020	36
0149-0426	male	fl/fl	+/T	27.06.2019	11.02.2020	33
0149-0451	male	fl/fl	+/+	10.07.2019	10.02.2020	31
0149-0452	male	fl/fl	+/+	10.07.2019	12.02.2020	31
0149-0453	male	fl/fl	+/T	10.07.2019	12.02.2020	31
0149-0454	male	fl/fl	+/+	10.07.2019	12.02.2020	31
0149-0486	male	fl/fl	+/T	25.07.2019	12.02.2020	29
0149-0487	male	fl/fl	+/T	25.07.2019	12.02.2020	29
0149-0488	male	fl/fl	+/+	25.07.2019	12.02.2020	29

Table S3: Animals used for ING3 staining.

Animal ID	Sex	*Ing3*	Pb-Cre4	Date of birth	Date of organ/ prostate harvest	Age (weeks)
0149-0419	male	fl/fl	+/T	05.06.2019	06.02.2020	35
0149-0425	male	fl/fl	+/+	27.06.2019	03.02.2020	32
0482-0142	male	+/+	+/+	03.08.2019	11.02.2020	27

Table S4: dPCR calibration instrument readout.

Animal ID	1 - (*Ing3*/*B2m*)	Copies/rxn (*Ing3*)	CI Copies/rxn (*Ing3*)	Copies/µl (*Ing3*)	Copies/rxn (*B2m*)	CI Copies/rxn (*B2m*)	Copies/µl (*B2m*)	Qualified partitions	Filled partitions
0117-0394	49.72%	0.356	0.346–0.367	471.79	0.708	0.693–0.725	938.3	15943	18773
0120-0172	-1.16%	0.736	0.719–0.752	974.48	0.727	0.711–0.744	963.31	15689	18180
NTC	93.96%	1.18E-04	2.95E-5–4.72E-4	0.156	1.95E-03	1.39E-3–2.74E-3	2.584	16931	18731
0120-0173	-0.88%	0.472	0.46–0.484	624.73	0.468	0.456–0.479	619.3	16924	18357
0120-0174	-0.71%	0.785	0.768–0.802	1039.8	0.78	0.763–0.797	1032.5	15859	17647
0120-0176	-3.87%	0.724	0.708–0.74	959.01	0.697	0.682–0.713	923.28	16742	17649
0149-0460	49.52%	0.247	0.238–0.256	327.16	0.489	0.476–0.503	648.1	14035	16142
0149-0461	99.91%	4.55E-04	2.17E-4–9.55E-4	0.603	0.526	0.513–0.54	697.15	15380	16556
0149-0462	50.89%	0.3	0.29–0.311	397.67	0.611	0.596–0.628	809.76	13042	15209
0149-0463	48.36%	0.154	0.148–0.16	204.12	0.298	0.29–0.307	395.29	16922	18340
0149-0464	49.36%	0.174	0.168–0.181	230.97	0.344	0.335–0.354	456.08	16563	18171
0149-0465	99.98%	1.19E-04	2.96E-5–4.74E-4	0.157	0.518	0.505–0.53	685.77	16876	17759
0149-0466	99.71%	1.61E-03	1.10E-3–2.37E-3	2.139	0.56	0.547–0.574	741.58	16113	18442
0149-0467	46.57%	0.165	0.157–0.173	218.12	0.308	0.297–0.32	408.23	9954	13911
0149-0468	99.99%	6.13E-05	8.63E-6–4.35E-4	8.11E-02	0.64	0.626–0.655	848.29	16327	17329
NTC	0.00%	5.85E-05	8.23E-6–4.15E-4	7.74E-02	5.85E-05	8.23E-6–4.15E-4	7.74E-02	17108	18122

CI: 95% confidence interval

NTC: no template control

Rxn.: reaction

Table S5: dPCR recombination experiment instrument readout.

Animal ID/ prostate lobe	1 - (*Ing3*/*B2m*)	Copies/rxn (*Ing3*)	CI Copies/rxn (*Ing3*)	Copies/µl (*Ing3*)	Copies/rxn (*B2m*)	CI Copies/rxn (*B2m*)	Copies/µl (*B2m*)	Qualified partitions	Filled partitions
0149-0417/AP	3.05%	0.513	0.501–0.526	679.97	0.53	0.517–0.542	701.37	17515	18612
0149-0417/VP	-7.00%	3.84E-01	0.373–0.394	507.98	3.58E-01	0.349–0.368	474.75	17094	18345
0149-0417/DLP	0.64%	0.683	0.668–0.698	904.48	0.687	0.673–0.702	910.28	17346	18241
0149-0418/AP	35.68%	0.513	0.501–0.525	679.45	0.798	0.781–0.814	1056.4	17616	18394
0149-0418/VP	8.22%	5.25E-02	4.92E-2–5.61E-2	69.538	5.72E-02	5.37E-2–6.09E-2	75.768	17311	18426
0149-0418/DLP	30.20%	0.376	0.365–0.387	497.92	0.539	0.525–0.552	713.4	15571	17440
0149-0452/AP	0.74%	1.147	1.125–1.169	1518.6	1.155	1.133–1.178	1529.9	17670	18386
0149-0452/VP	-1.84%	0.595	0.582–0.609	788.19	0.584	0.571–0.598	773.92	17201	18359
0149-0452/DLP	4.86%	0.621	0.607–0.635	822.3	0.653	0.638–0.667	864.28	17973	18609
0149-0454/AP	-1.87%	0.853	0.835–0.871	1129.5	0.837	0.819–0.855	1108.8	15832	18029
0149-0454/VP	-9.26%	0.127	0.121–0.132	167.74	0.116	0.111–0.121	153.52	16314	17901
0149-0454/DLP	1.19%	0.471	0.459–0.483	623.33	0.476	0.464–0.489	630.82	16296	18156
0149-0486/AP	19.92%	0.448	0.436–0.459	593.06	0.559	0.546–0.573	740.61	16386	18230
0149-0486/VP	22.54%	0.298	0.29–0.308	395.31	0.385	0.375–0.396	510.33	16718	18270
0149-0486/DLP	25.04%	1.094	1.073–1.116	1449.2	1.46	1.432–1.488	1933.4	17166	18606
NTC	-600.48%	4.38E-04	2.09E-4–9.18E-4	0.58	6.25E-05	8.81E-6–4.44E-4	8.28E-02	15995	17953
0149-0453/AP	20.42%	0.541	0.528–0.554	716.78	0.68	0.665–0.695	900.76	16960	18230
0149-0453/VP	19.78%	0.46	0.448–0.472	609.05	0.573	0.56–0.587	759.22	16845	17899
0149-0453/DLP	19.75%	0.352	0.342–0.361	465.57	0.438	0.427–0.449	580.16	17289	18653
0149-0487/AP	11.50%	0.405	0.394–0.416	536.16	0.457	0.446–0.469	605.84	15951	17965
0149-0487/VP	27.51%	1.77	1.734–1.807	2343.9	2.441	2.387–2.496	3233.3	16115	17670
0149-0487/DLP	26.15%	0.322	0.313–0.332	426.79	0.436	0.425–0.448	577.89	16991	18389
0149-0488/AP	0.55%	0.827	0.81–0.845	1095.7	0.832	0.814–0.85	1101.8	16275	17838

Animal ID/ prostate lobe	1 - (*Ing3*/*B2m*)	Copies/rxn (*Ing3*)	CI Copies/rxn (*Ing3*)	Copies/µl (*Ing3*)	Copies/rxn (*B2m*)	CI Copies/rxn (*B2m*)	Copies/µl (*B2m*)	Qualified partitions	Filled partitions
0149-0488/VP	-1.43%	0.246	0.238–0.254	325.26	0.242	0.234–0.25	320.66	16602	18340
0149-0488/DLP	-1.78%	0.636	0.622–0.651	842.55	0.625	0.611–0.639	827.82	17038	18558
0149-0426/AP	27.72%	0.369	0.359–0.38	488.79	0.511	0.498–0.524	676.24	15428	18410
0149-0426/VP	27.65%	0.186	0.18–0.193	246.82	0.258	0.25–0.266	341.13	17815	18447
0149-0426/DLP	24.14%	0.425	0.414–0.436	562.69	0.56	0.547–0.574	741.75	16351	18006
0149-0451/AP	-0.75%	0.613	0.599–0.626	811.47	0.608	0.595–0.622	805.44	17999	18863
0149-0451/VP	-3.20%	0.401	0.391–0.412	531.4	0.389	0.379–0.399	514.9	17718	18501
0149-0451/DLP	-1.79%	0.53	0.518–0.543	702.22	0.521	0.509–0.533	689.9	17371	18898
NTC	0.00%	2.93E-04	1.22E-4–7.04E-4	0.388	2.93E-04	1.22E-4–7.04E-4	0.388	17074	17703

CI: 95% confidence interval

NTC: no template control

Rxn.: reaction

AP: anterior prostate

VP: ventral prostate

DLP: dorsolateral prostate

Grey highlight: chip excluded from statistical analysis (copy count out of dynamic range)

11 Acknowledgements

First of all, I would like to express my sincere gratitude to my supervisor Dr. Dieter Fink for his unparalleled support and patient guidance. Special thanks to Dr. Thomas Rülicke for allowing me to pursue my thesis project as a part of his team.

I particularly want to thank Dr. Ralf Steinborn and Martin Hofer, BSc, for their invaluable contributions in the set-up and establishment of the dPCR assay. Furthermore, I would like to acknowledge the help of Dr. Bettina Wagner and MMag. Barbara Pachner in the lab.

I am deeply grateful to Dr. Karl Riabowol and Karen Blote, MSc, for welcoming me at the Riabowol Laboratory, University of Calgary, and their assistance in performing the immunohistochemical staining.

Finally, I want to extend my thanks to my friends and family who always supported and encouraged me during my studies.